JOURNAL OF MATERIALS SCIENCE 29 (1994) 4043–4050

Effective medium theory and the thermal conductivity of plasma-sprayed ceramic coatings

A. BJORNEKLETT, L. HAUKELAND, J. WIGREN*, H. KRISTIANSEN
SINTEF SI, P.O. Box 124 Blindern, N-0314 Oslo, and also Department of Physics, University of Oslo, P.O. Box 1048 Blindern, N-0316 Oslo, Norway
**Volvo Flygmotor AB, Aerospace Division, S-461 81 Trollhättan, Sweden*

The thermal diffusivity of plasma-sprayed zirconium oxide–7% yttrium oxide and aluminium oxide–3% titanium oxide ceramic coatings was measured by using a periodic heat-flow method. Samples were prepared with different porosities thus allowing the thermal diffusivity as function of porosity to be determined. The samples were also impregnated with silicone oil so that the effect on the thermal diffusivity by replacing air with silicone oil in the pores could be determined. The experimental results were compared with effective medium theories representing three different microstructures: (1) a continuous ceramic matrix with dispersed pores, (2) a continuous ceramic matrix with continuously interconnected pores, (3) dispersed ceramic particles loosely bonded together. The latter two microstructures gave the best agreement between the experimental data and the theory.

1. Introduction

Plasma-sprayed ceramic coatings have been used for wear and corrosion protection and thermal barriers for the last 30 years [1]. In recent years, some attempts to use plasma-sprayed coatings as dielectric material in electronic packages have been made [2, 3]. This application promises highly cost-effective production in high volumes and at least one successful product has been reported so far [4]. The thermal conductivity of plasma-sprayed coatings is of considerable importance both in thermal barrier and electronic packaging applications. Thermal barriers should have a low thermal conductivity and electronic packages a high thermal conductivity.

Reported measurements of thermal conductivity in plasma-sprayed ceramic coatings show large variations [5]. One reason for this is probably the difficulty of performing such measurements. Differences in the microstructure in these coatings certainly also influence the spread in the thermal conductivity results. Thermal conductivity is usually found to be considerably less than that of sintered materials of equal composition, but without pores. Values as low as 1% of the bulk value have been reported [6], as also have values as high as 50% [7].

The phase composition of the coating is reported to play an important role in thermal conductivity [7]. Plasma spraying is a rapid solidification process and the coatings may consist of metastable phases that have different thermal properties from the thermodynamically stable phases. For instance, the main constituent of plasma-sprayed aluminium oxide is reported to be the γ-phase [7]. The low thermal conductivity of plasma-sprayed alumina coatings compared to sintered alumina was assumed to be associated with a lower thermal conductivity of the γ-phase. On heating the alumina coating to 1500 K the γ-phase transforms to the thermodynamically stable α-phase and a two- to three-fold increase in thermal conductivity is observed. (Some of this effect may be due to closure of pores in the coating.) Coatings produced by using a short distance between the plasma gun and the substrate or by spraying on to preheated substrates, contain a substantial amount of α-phase with a higher thermal conductivity [7].

Porosity is another important parameter with a significant influence on the thermal conductivity of plasma-sprayed coatings. The porosity of ceramic coatings is typically around 10%. The effect of porosity on the thermal conductivity depends strongly on the shape and connectivity of the pores. There is some evidence that the pores in ceramic coatings are lamellar regions separating the liquid droplets during coating formation. The thickness of these regions is 0.01–0.1 μm [8].

This paper reports measurements of the thermal diffusivity of zirconium oxide–7% yttrium oxide and aluminium oxide–3% titanium oxide coatings with various porosities before and after impregnation with silicone oil. The effect of replacing air with silicone oil in the pores has a technological significance. In some electrical applications the coatings are impregnated with an organic sealer in order to increase the dielectric strength of the coating [3, 4]. In addition to

0022–2461

investigating the effect of silicone oil impregnation on thermal conductivity, the main purpose of the present study was to investigate the microstructure of the coatings by comparing the measured thermal conductivity with that predicted from effective medium theories, representing different geometries and connectivity of the pores.

2. Thermal conductivity of two-phase materials

A porous plasma-sprayed ceramic coating is a mixture of ceramic and air. Macroscopic mixtures of two or more different materials, often called composite materials, are common in technology and several theories have been developed to explain the transport properties of such materials. The first theoretical developments in this subject, often called the effective medium theory were made by Maxwell *et al.* [9]. Recently, McLachlan introduced a general effective medium theory that also includes the results from percolation theory [13].

In order for the effective medium theory to be applicable for composite materials, it must be described by characteristic parameters. One important set of parameters is the relative amounts (volume fractions) of the different phases. This would be the fraction of pores in the case of a ceramic coating. However, the porosity alone is not sufficient to characterize a composite material. The shape, orientation and distribution of the pores are equally important. If, for instance, the pores are shaped as thin lamellae, oriented perpendicular to the heat flow, they would have a far stronger effect on the thermal conductivity than if they were spherical.

The connectivity of the phases is also a key feature of composite materials [14]. For instance, a polymer filled with metal particles may have a 3–0 or a 3–3 connectivity depending on whether or not the metal particles build a conductive network [15]. The first number (3) indicates that the polymer is selfconnected in all three directions because it is the matrix. The second number (3 or 0) indicates in how many directions the metal particles are selfconnected. In many cases the connectivity is of physical importance because it determines whether or not the mixture is electrically conductive.

Fig. 1 depicts three possible connectivity schemes of a plasma-sprayed ceramic coating. The first is a 3–0 medium equivalent to unconnected pores in a continuous ceramic matrix. The 3–3 media have interconnected networks of both ceramic and pores. The 0–3 connectivity is strictly not possible, because the ceramic grains would fall apart. However, if the ceramic grains are thought of as being interconnected only at a few tiny spots, the medium could be considered to be a quasi 0–3 medium. Media with different connectivities of the phases are asymmetrical and media with equal connectivities are symmetrical.

Asymmetrical isotropic media have a 3–0 or 0–3 connectivity. A common effective medium theory describing the thermal conductivity and other physical

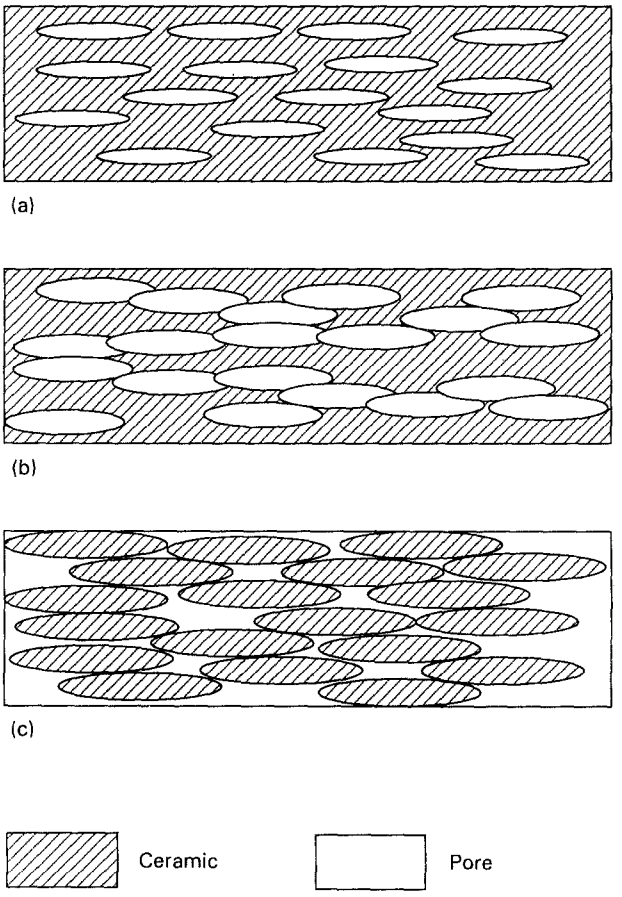

Figure 1 Visualizations of three different connectivities in a plasma-sprayed ceramic coating. (a) Asymmetrical medium, 3–0 connectivity; (b) symmetrical medium, 3–3 connectivity; (c) asymmetrical medium, 0–3 connectivity.

properties of such media was introduced by Garnet [10, 11]. The thermal conductivity of a mixture of unconnected grains with thermal conductivity k_D dispersed in a matrix with thermal conductivity k_M, is given as

$$k_C = k_M \frac{Lk_D + (1-L)k_M + f(1-L)(k_D - k_M)}{Lk_D + (1-L)k_M - fL(k_D - k_M)} \quad (1)$$

where f is the volume fraction of the dispersed phase. This equation is the general form of the Maxwell theory with oriented ellipsoidal grains. L is the depolarization factor of the ellipsoids in the direction of heat flow [16]: $L = 1/3$ for spherical grains; $1/3 > L > 0$ for prolate ellipsoids; $1 > L > 1/3$ for oblate ellipsoids. If the dispersed phase is non-conductive and f is small (e.g. pores in a ceramic material) then the dilute limit of the Maxwell equation is given as

$$k_C = k_M\left(1 - \frac{f}{1-L}\right) \quad (2)$$

This equation is only valid for 3–0 media.

The Bruggeman symmetric effective medium theory [12] applies to media with 3–3 connectivity. A symmetrical medium may be visualized as being built up

from ellipsoids of both phases, completely filling the medium. An infinite size range of ellipsoids is thus necessary to fill the entire medium. The thermal conductivity of such a medium may be calculated from the Bruggeman equation

$$f\frac{k_1 - k_C}{k_C + L_1(k_1 - k_C)} + (1-f)\frac{k_2 - k_C}{k_C + L_2(k_2 - k_C)} = 0 \quad (3)$$

where k_1, k_2 and k_C are the thermal conductivities of phase 1, phase 2 and the composite, respectively, the volume fraction of phase 1 being f and the depolarization factors of the ellipsoids of phases 1 and 2 being L_1 and L_2, respectively.

3. Experimental procedure

Plasma-sprayed ceramic coatings of zirconium oxide–7% yttrium oxide (ZrO_2 + 7% Y_2O_3) and aluminium oxide–3% titanium oxide (Al_2O_3 + 3% TiO_2) with different porosities were made by Volvo Flygmotor AB. Five zirconia and two alumina samples were included in the study. The zirconia samples were made from agglomerated and sintered powder. The substrate material was Hastelloy X, a nickel-based superalloy, and NiCrAlY was used as bond layer. The alumina sample with the highest porosity was sprayed on to Inconel 718 substrate and the other sample on to titanium. The bond layer was NiAl for both samples. Different porosities were obtained by varying the spray parameters in the case of the zirconia samples and by using two different powder sizes in the case of the alumina samples. The plasma-spray equipment was a Metco 9M gun. To enable measurements of the thermal diffusivity of the coatings they were separated from the substrate, then cleaned and dried. The porosity of the zirconia coatings was measured by a water intrusion technique at Volvo Flygmotor AB. The porosity of the alumina coatings was measured by an image analysis technique at SINTEF SI. The fraction of pores in five frames of 100 μm × 100 μm dimension was recorded for each sample. The minimum pore size that was detected was 1 μm.

Before the samples were subjected to measurement, they were baked at 130 °C for 24 h in order to remove any adsorbed water. After the first measurements, the samples were submersed in silicone oil (Dow Corning 200 fluid) for 70 h at 70 °C in order to fill the pores with a material of different thermal conductivity than air.

The thermal diffusivity of the coatings was measured with a periodic heat-flow method. The basic theory of the method was first described by Ångström [17]. In our implementation of the method, a light source with a computer-controlled shutter irradiates the sample. The shutter opens and closes the light path periodically, thus inducing thermal waves in the sample. A thermocouple measures the temperature on the sample. A computer-controlled mask constricts the irradiating light so that the distance between the irradiated area and the temperature measurement position may be changed, see Fig. 2. The amplitude of the

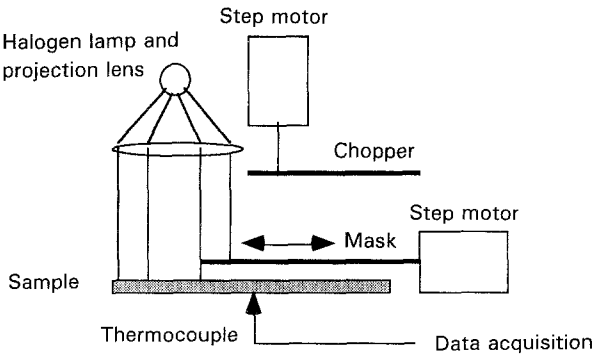

Figure 2 Schematic outline of the equipment used for thermal diffusivity measurements.

thermal waves is given as [18]

$$T_{amp} = T_0 \exp\left[-\left(\frac{\pi f}{a}\right)^{1/2} x\right] \quad (4)$$

where a is the thermal diffusivity, f is the chopping frequency of the irradiated light and x is the distance between the temperature measurement position and the irradiated area. In practice, the temperature amplitude was measured at several different positions and a straight line was least-square fitted to the natural logarithm of the temperature amplitude as function of position

$$\ln\left(\frac{T_{amp}}{T_0}\right) = A + Bx \quad (5)$$

The thermal diffusivity is then given as

$$a = \frac{\pi f}{B^2} \quad (6)$$

The distance between the thermocouple and the irradiated area was changed by moving the irradiated area using the movable mask rather than moving the thermocouple. Inaccuracies caused by variation in thermocouple contact resistance were thus avoided. Calibration of the thermocouple was superfluous because only relative measurements are needed. The frequency, f, used in this study was 0.4 Hz.

The temperature was sampled by a computer 64 times in each period and the amplitude was extracted by a digital filtering technique. We estimate the accuracy of the measurements to be approximately ± 5% for the alumina samples and ± 10% for the zirconia samples. The uncertainty was mainly due to inhomogeneous optical absorption in the samples, mechanical instabilities in the mask and thermal noise and drift that mainly affected measurements on samples with low thermal diffusivity. The thermal conductivity of the samples was calculated from

$$k = a\rho C_p \quad (7)$$

where ρ is the density and C_p the heat capacity, see Table I [19]. The heat capacity of the ceramic samples was measured with a Perkin–Elmer DSC7 (differential scanning calorimeter). The density was corrected for the porosity in the samples and C_p was corrected for the presence of silicone oil in the porosities.

TABLE I Density and specific heat capacity of zirconium oxide/yttrium oxide, aluminium oxide/titanium oxide and silicone oil used in the calculation of thermal conductivity from measurements of thermal diffusivity

Material	ρ (kg m^{-3})	C_p (J kg^{-1} K^{-1})
Zirconia	6100	457
Alumina	3900	831
Silicone	970	1490

4. Results and discussion

The porosities, thermal diffusivities and calculated conductivities of the samples before and after impregnation with silicone oil are given in Table II. The measured thermal diffusivities and corresponding thermal conductivities are in reasonable agreement with previously reported results. The thermal conductivities in zirconia coatings have previously been reported to be from 0.45–1.8 W m^{-1} K^{-1} [5] and the thermal conductivities in alumina titania coatings from 2–6 W m^{-1} K^{-1} [20]. The measured value of the heat capacity, C_p, of zirconium oxide/yttrium oxide coating was in excellent, agreement with the tabulated value for pure zirconium oxide [19]. The measured value for aluminium oxide/titanium oxide was 7% higher than tabulated for pure aluminium oxide [19]. However, these C_p measurements disagree with values obtained at Volvo Flygmotor by separately measuring the thermal diffusivity and the thermal conductivity with a laser pulse technique. The C_p was calculated from Equation 7 and was approximately a factor two to three times higher than the differential scanning calorimeter (DSC) result. It was decided to use the DSC results in this study because they gave the best agreement with tabulated values [19]. However, it is possible that plasma-sprayed coatings may have a different C_p than similar sintered materials due to a different phase composition.

Effective medium theories for thermal conductivity representing three different connectivity schemes or microstructures were fitted to the data. The Maxwell–Garnet theory, Equation 1, was used in the case of asymmetrical media with 3–0 or 0–3 connectivities. The symmetrical theory of Bruggeman, Equation 3, was used for the medium with 3–3 connectivity. The idea was to investigate how well the different theories fit the experimental data and from that draw some conclusions about the microstructure of the ceramic coatings. Thermal conductivity in pure coatings and in coatings impregnated with silicone oil were both used when the theories were fitted to the data. In this way the parameters in the theories were more constrained than if only one part of the data set was used, thereby giving a more complete theoretical description. It was assumed that the silicone oil penetrated all the pores and that the geometrical shape of the pores was similar whether they were filled with air or silicone oil. The thermal conductivity was assumed to be 0.026 W m^{-1} K^{-1} for air and 0.12 W m^{-1} K^{-1} for silicone oil [17].

Fig. 3 shows a best fit plot of the Maxwell–Garnet effective medium theory and the experimental results for zirconia. In this plot it is assumed that there is a 3–0 connectivity in the coating. The sum of the squared differences between theoretical and experimental results has been minimized by varying the thermal conductivity of the zirconia matrix and the depolarization factor, L. It should be stressed that

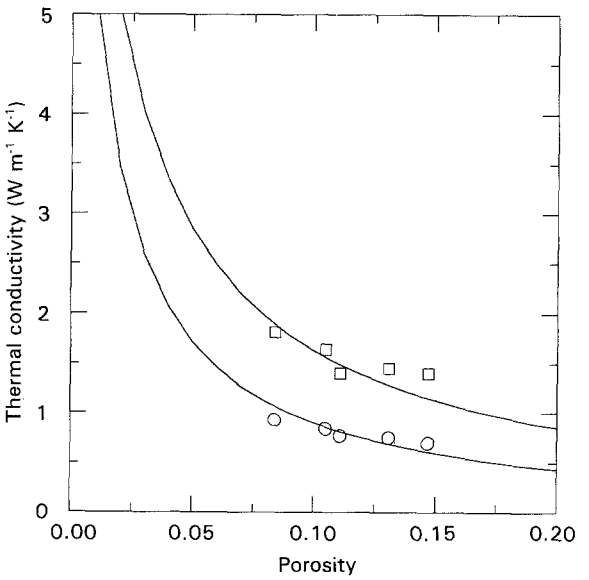

Figure 3 Best fit of Maxwell–Garnet asymmetrical effective medium theory to the experimental results for zirconium oxide/yttrium oxide (□) with and (○) without silicone oil. The curves start at 10.35 W m^{-1} K^{-1} for 0 porosity. The sum of quadratic deviations is 0.145 (W m^{-1} K^{-1})^2.

TABLE II Porosities, f, thermal diffusivities, a, before and after silicone oil impregnation (Dow Corning 200 fluid). The thermal conductivity, k, is calculated from Equation 7 and the data given in Table I. Z-1-5 designate the zirconium oxide/yttrium oxide samples and A-1-2 the aluminium oxide/titanium oxide samples

Sample	f	Before impregnation		After impregnation	
		a (mm^2 s^{-1})	k (W m^{-1} K^{-1})	a (mm^2 s^{-1})	k (W m^{-1} K^{-1})
Z-1	0.084	0.365	0.93	0.675	1.81
Z-2	0.105	0.335	0.84	0.620	1.64
Z-3	0.111	0.310	0.77	0.530	1.40
Z-4	0.131	0.310	0.75	0.550	1.45
Z-5	0.147	0.290	0.70	0.540	1.40
A-1	0.040	1.11	3.45	1.45	4.60
A-2	0.082	1.06	3.15	1.35	4.18

both the results before and after impregnation with silicone oil were used to obtain the optimal theoretical parameters. Fig. 4 shows a similar best fit plot of the Bruggeman symmetrical theory. In this theory there are three parameters that have been varied, the thermal conductivity of dense zirconia and the depolarization factor of both the zirconia and the pore phase. Fig. 5 shows the Maxwell–Garnet theory for a 0–3 connected medium with zirconia grains embedded in air or silicone oil. Figs 6–8 show similar plots for the alumina–titania coating. Table III gives the parameters and the sum of the square deviations between the experimental and the theoretical results.

The depolarization factors reflect the shape of the dispersed pores or particles. Plasma-sprayed ceramic coatings are built up from splashes of molten ceramic droplets. Therefore, the depolarization factor of the ceramic phase was expected to be in the interval (0, 1/3) in the lateral direction and in the interval (1/3, 1) in the direction normal to the coating. The depolarization factors for the ceramic phase with a best fit to the experimental results, were 0.043 and 0.165 for zirconia and 0.000 and 0.035 for alumina in the 3–3 and 0–3 medium, respectively. The measurements were made in the lateral direction thus confirming the expectation. This of course also indicates that ceramic coatings have anisotropic thermal transport properties which have been experimentally confirmed in another investigation [21]. A depolarization factor

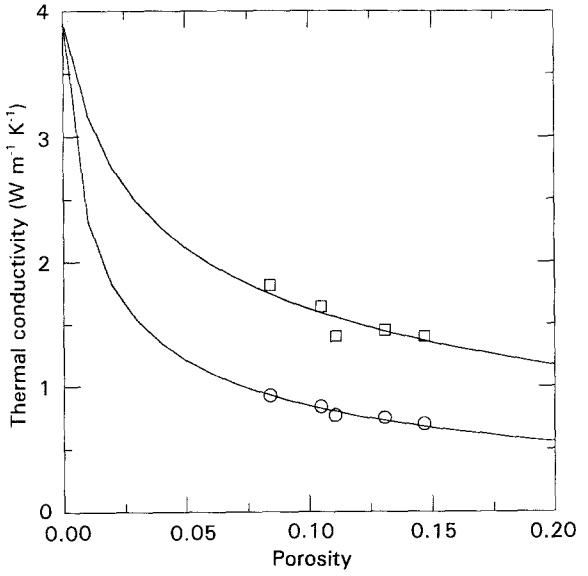

Figure 4 Best fit of Bruggeman's symmetrical effective medium theory to the experimental results for zirconium oxide/yttrium oxide (□) with and (○) without silicone oil. The sum of quadratic deviations is 0.032 $(W m^{-1} K^{-1})^2$.

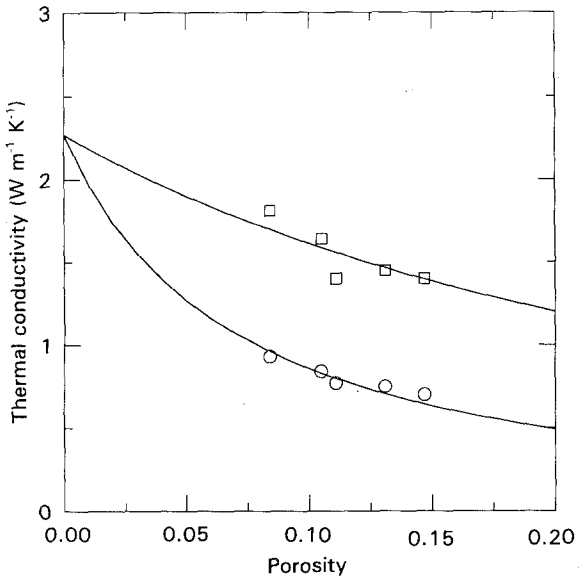

Figure 5 Best fit of Maxwell–Garnet asymmetrical effective medium theory to the experimental results for zirconium oxide/yttrium oxide (□) with and (○) without silicone oil. The sum of quadratic deviations is 0.048 $(W m^{-1} K^{-1})^2$.

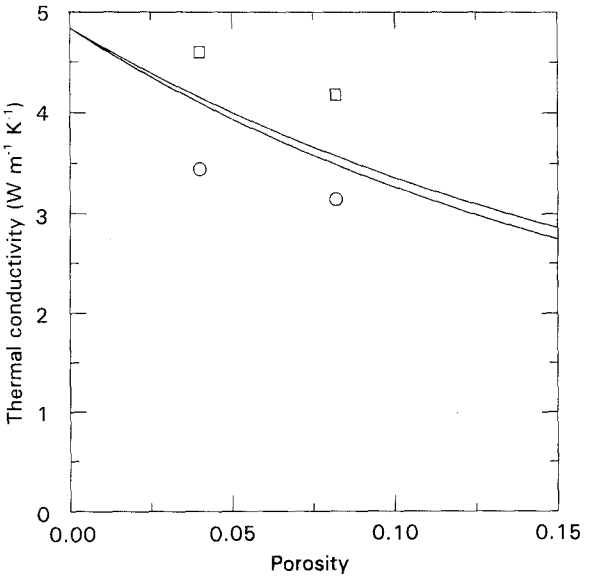

Figure 6 Best fit of Maxwell–Garnet asymmetrical effective medium theory to the experimental results for aluminium oxide/titanium oxide (□) with and (○) without silicone oil. The sum of quadratic deviations is 1.103 $(W m^{-1} K^{-1})^2$.

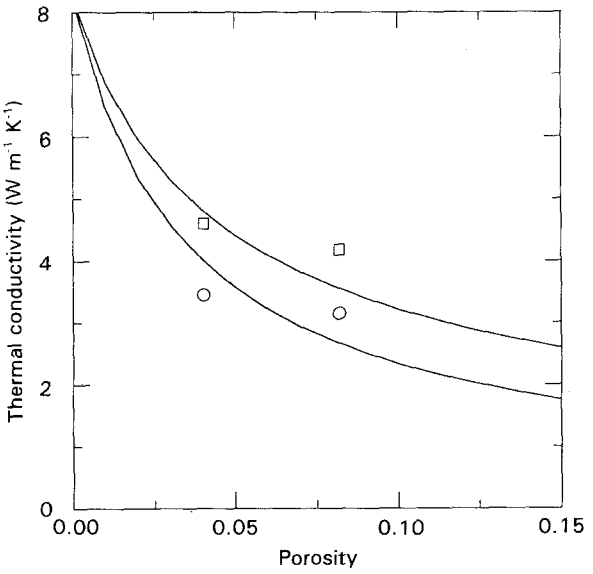

Figure 7 Best fit of Bruggeman's symmetrical effective medium theory to the experimental results for aluminium oxide/titanium oxide (□) with and (○) without silicone oil. The sum of quadratic deviations is 0.977 $(W m^{-1} K^{-1})^2$.

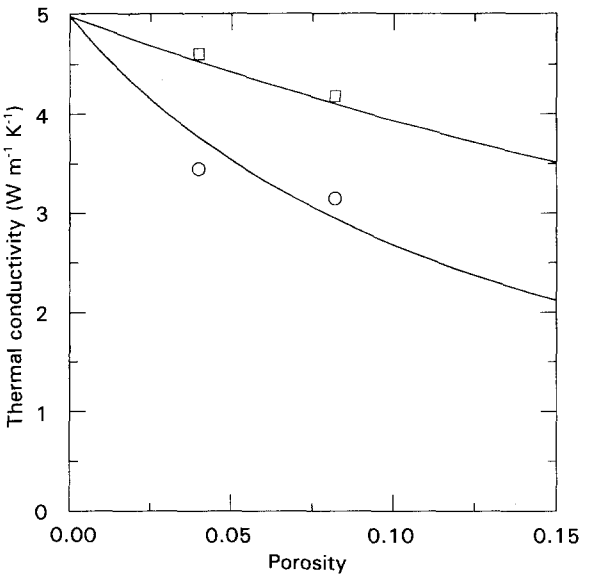

Figure 8 Best fit of Maxwell–Garnet asymmetrical effective medium theory to the experimental results for aluminium oxide/titanium oxide (□) with and (○) without silicone oil. The sum of quadratic deviations is 0.151 $(W m^{-1} K^{-1})^2$.

TABLE III Effective medium parameters giving a best fit of experimental and theoretical results. k_{zirc} and k_{alu} are the thermal conductivity of dense zirconium oxide/yttrium oxide and aluminium oxide/titanium oxide, L_{pore}, L_{zirc} and L_{alu} are the depolarization factors of the pores and the ceramic ellipsoids. Σ_{dev} is the sum of the squared differences between theoretical and experimental results. MG designates Maxwell–Garnet theory and BR Bruggeman theory

	MG, 3–0	BR, 3–3	MG, 0–3
Zirconium oxide/yttrium oxide			
k_{zirc} $(W m^{-1} K^{-1})$	10.35	3.91	2.27
L_{pore}	0.992	0.996	–
L_{zirc}	–	0.043	0.165
Σ_{dev} $(W m^{-1} K^{-1})^2$	0.048	0.145	0.032
Aluminium oxide/titanium oxide			
k_{alu} $(W m^{-1} K^{-1})$	4.84	8.22	4.97
L_{pore}	0.774	0.967	–
L_{alu}	–	0.000	0.035
Σ_{dev} $(W m^{-1} K^{-1})^2$	1.103	0.977	0.151

equal to zero corresponds to infinitely long fibres or rods in the direction of heat flow. In the 3–0 medium there is no depolarization factor associated with the ceramic phase because it is the matrix phase.

The shape of the pores was more uncertain, but previously published work indicates that the pores are of lamellar shape separating the ceramic droplets [8]. The experimentally determined depolarization factors for the pores were 0.996 and 0.992 for zirconia and 0.967 and 0.774 for alumina in the 3–3 and 3–0 media, respectively. These figures indicate that the pores are strongly oblate in the direction of heat flow. Pores which are oblate in the heat-flow direction have a much stronger impact on the thermal conductivity than pores that are elongated in the same direction. In a ceramic coating with randomly distributed lamellar pores, the effective depolarization factor will be larger than 1/3 because the pores that are oblate in the direction of heat flow will dominate the reduction of thermal conductivity of the coating. The observed depolarization factors may thus be explained by a random distribution of lamellar pores. In the 0–3 medium model, there is no depolarization factor of the pores because they constitute the matrix phase. The major problem with the 0–3 model is the fact that the ceramic grains are unconnected which obviously is not the case, because the coating would not be solid. In our opinion the ceramic coating should be described by an effective medium model that takes care of the fact that both the ceramic and the pore phase are interconnected. However, the connectivity of the ceramic phase does not necessarily have to be strong. This is also in agreement with a model developed by McPherson [5] where one-fifth of the area of the flake-like ceramic particles were connected to other particles.

The agreement between the experimental data and theories is best for 3–3 and 0–3 media. In the case of zirconia, the square deviation for the 3–0 medium is at least three times as high as for the other theories. The alumina samples show best agreement with the 0–3 and worst with the 3–0 model. However, an additional argument is the unrealistically high thermal conductivity of solid zirconia implied by the 3–0 medium. The best fit curves gave a thermal conductivity of 10.35 $W m^{-1} K^{-1}$. It is reported that the thermal conductivity of zirconia coatings increases three to four times upon heating to 2200 K [5]. This effect is attributed to closure of the typical lamellar pores, resulting in a dense coating with thermal conductivity of approximately 2 $W m^{-1} K^{-1}$. This value is in reasonable agreement with the 3–3 and 0–3 media models, assuming that some porosity was still present in heated samples.

Fig. 9 shows cross-sections of the zirconia samples. Large and more or less spherical pores of up to 10 μm diameter are easily visible. There are also a network of fine dark lines randomly oriented, that may represent lamellar pores up to 1 μm thick. These structures are most easily seen on samples Z-1 and Z-2 which have the lowest porosities. Only the largest lamellar pores are observable with optical microscopy. The limited resolution may, therefore, hide more lamellar pores. Electron microscopy, however, did not provide any further information regarding lamellar pores with thickness below 1 μm.

The alumina data are not as significant as the zirconia data because only two different porosities were available and also because the measurement of porosity only included pores larger than 1 μm. Lamellar pores with dimensions less than 1 μm were not included, but these pores are probably the most important ones regarding thermal conductivity. Fig. 10 show cross-sections of the alumina samples. It is evident that sample A-2 has a higher porosity than sample A-1. However, the difference in thermal conductivity between A-1 and A-2 was much smaller than expected from the difference in porosity thus indicating that the samples were more similar on a microscopic scale. The thermal conductivity of dense

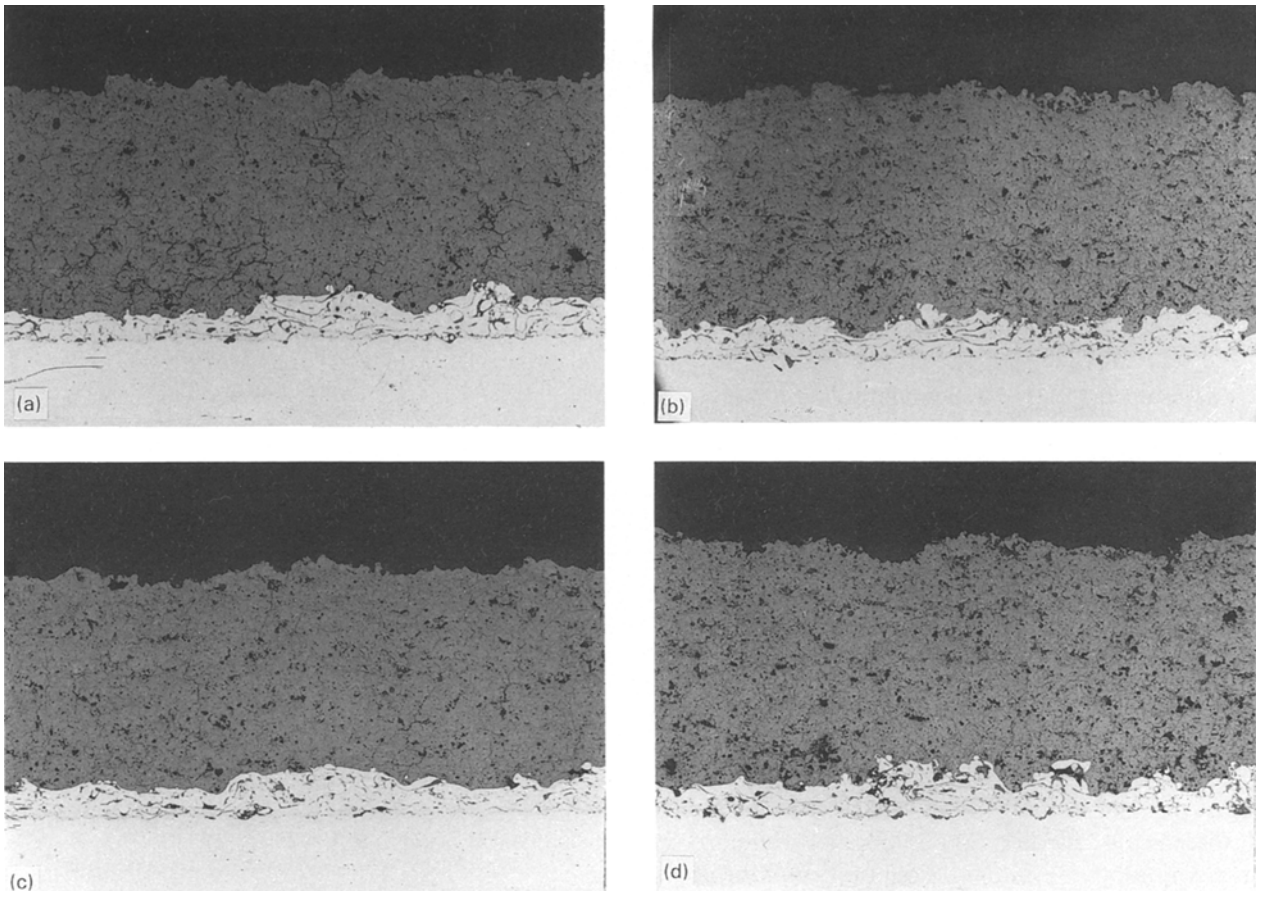

Figure 9 (a–e) Cross-sections of (a) samples Z-1 to (e) Z-5 before separation from the substrate. × 100

alumina predicted by the effective medium theories was also too low. Dense sintered alumina typically has a thermal conductivity in the 20–30 $W m^{-1} K^{-1}$ range. We suggest that there were more pores in samples A-1 and A-2 than measured and that these pores are of the thin lamellar type. Such pores could not be detected due to the limited resolution power of the image analyser used for porosity measurement.

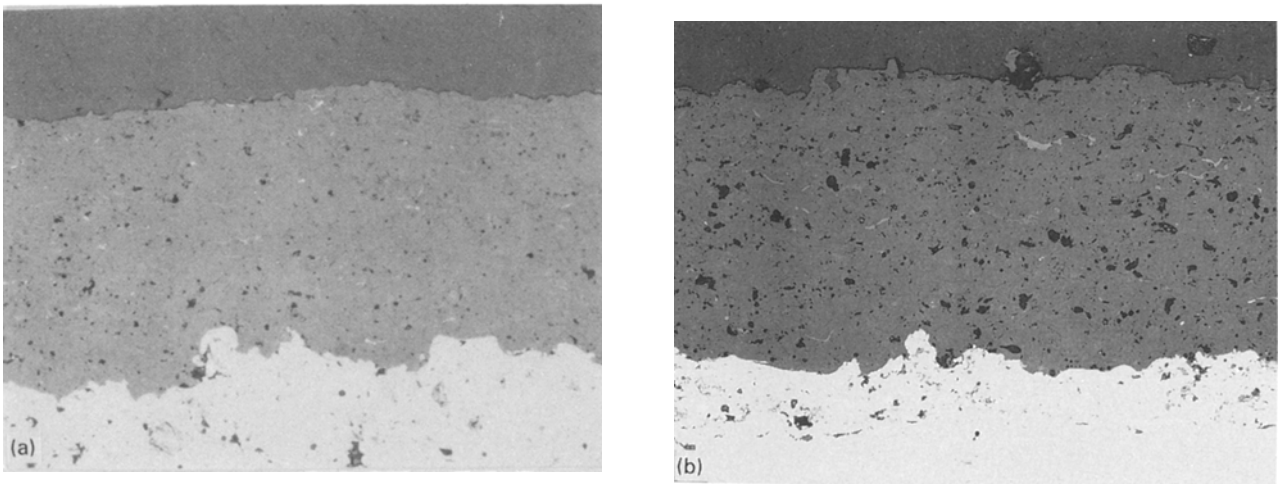

Figure 10 Cross-sections of (a) samples A-1 and (b) A-2 before separation from the substrate. × 100

5. Conclusion

The thermal diffusivity of plasma-sprayed ceramic coatings of zirconium oxide–7% yttrium oxide and aluminium oxide–3% titanium oxide was measured before and after impregnation with silicone oil. A considerable increase in thermal diffusivity (100% for ZrO and 35% for Al_2O_3) was found after impregnation. The experimental data were compared to effective medium models representing three different connectivity schemes. The models with 3–3 and 0–3 connectivities conformed best to the experimental data. The thermal conductivity of dense zirconium oxide predicted by the 3–0 model was too high to be realistic. Thus a plasma-sprayed ceramic coating behaves more like an agglomerate of ceramic particles than a solid ceramic sheet with pores, with respect to thermal diffusivity and conductivity.

The formation process of plasma-sprayed coatings also supports a 3–3 or 0–3 description. Molten or partially molten ceramic particles impinge on to the substrate where they splash out into circular discs before they freeze in less than a microsecond. If a major part of the area of the particles is sintered together the resulting medium would be a 3–0 medium. If the particles are sintered together at a few spots the resulting medium would be of the 3–3 type. If there is only mechanical bonding between particles then a quasi 0–3 medium description could be applied. Owing to the rapid solidification in plasma-sprayed coatings it is difficult to believe that most of the particle areas are sintered together. This leaves the 3–3 and quasi 0–3 descriptions as the most probable ones.

Acknowledgements

The authors thank Leif Halbo for helpful comments and Irene F. Sveen for the image analysis of samples A-1 and A-2. Financial support from the Royal Norwegian Council for Scientific and Industrial Research (NTNF) to one of us (A.B.) is gratefully acknowledged.

References

1. J. H. ZAAT, *Ann. Rev. Mater. Sci.* **13** (1983) 9.
2. R. H. PALMER, in "Proceedings of the 13th International Thermal Spraying Conference", edited by C. C. Berndt (ASM, Materials Park, Ohio, 1992) p. 825.
3. A. BJORNEKLETT, L. M. NILSEN, H. KRISTIANSEN and T. STORFOSSENE, *ibid.*, p. 829.
4. T. PETERMAN, *ibid.*, p. 309.
5. R. MCPHERSON, *Thin Solid Films* **112** (1984) 89.
6. J. GERARD-HIRNE and Y. LAZENNEC, *Trans. Int. Ceram. Congr.* **10** (1967) 413.
7. H. C. FIEDLER, *Mater. Res. Soc. Symp. Proc.* **30** (1984) 173.
8. R. McPHERSON and B. V. SHAFER, *Thin Solid Films* **97** (1982) 201.
9. J. C. MAXWELL, "A Treatise on Electricity and Magnetism", 3rd Edn (Dover, New York, 1954) Ch. 9.
10. J. GARNET, *Phil. Trans. R. Soc. Lond.* **203** (1904) 385.
11. *Idem, ibid.* **205** (1906) 237.
12. D. BRUGGEMAN, *Ann. Phys.* **24** (1935) 636.
13. D. S. McLACHLAN, *J. Phys. C Solid State Phys.* **20** (1987) 865.
14. R. E. NEWHAM, D. P. SKINNER and L. E. CROSS, *Mater. Res. Bull.* **13** (1978) 525.
15. A. BJORNEKLETT, L. HALBO and H. KRISTIANSEN, *Int. J. Adhesion Adhesives* **12** (1992) 99.
16. P. N. SEN, C. SCALA and M. H. COHEN, *Geophys.* **46** (1981) 781.
17. A. J. ÅNGSTRÖM, *Ann. Phys. Chem.* **64** (1861) 33.
18. B. SUNDQVIST, *Int. J. Thermophys.* **12** (1991) 191.
19. D. R. LIDE, "CRC Handbook of Chemistry and Physics", 73rd Edn (CRC Boca Raton, Fl, 1992).
20. L. PAWLOWSKI, C. MARTIN and P. FAUCHAIS, in "Proceedings of the 10th International Thermal Spraying Conference" (Deutscher Verlag Fur Schweisstechnik (DVS) GmbH, Dusseldorf, 1983) p. 31.
21. H. NAKAHIRA, K. TANI, K. MIYAJIMA and Y. HARADA, in "Proceedings of the 13th Int. Thermal Spraying Conference", edited by C. C. Berndt (ASM, Materials Park, Ohio, 1992) p. 1011.

Received 9 February 1993
and accepted 28 January 1994